Electronic Supplementary Material (ESI) for Nanoscale.
This journal is © The Royal Society of Chemistry 2023

SUPPORTING INFORMATION

Yttrium Preintercalated Layered Manganese Oxide as a Durable Cathode for Aqueous Zinc−Ion Batteries

Tzu−Ho Wu*, Ya−Qi Lin, Jian-Xue Huang

Department of Chemical and Materials Engineering, National Yunlin University of Science and Technology, Yunlin 64002, Taiwan

*Corresponding author: Tzu−Ho Wu, Assistant Professor
E−mail: wutzu@yuntech.edu.tw
Website: https://tzuhowu.wixsite.com/eelab

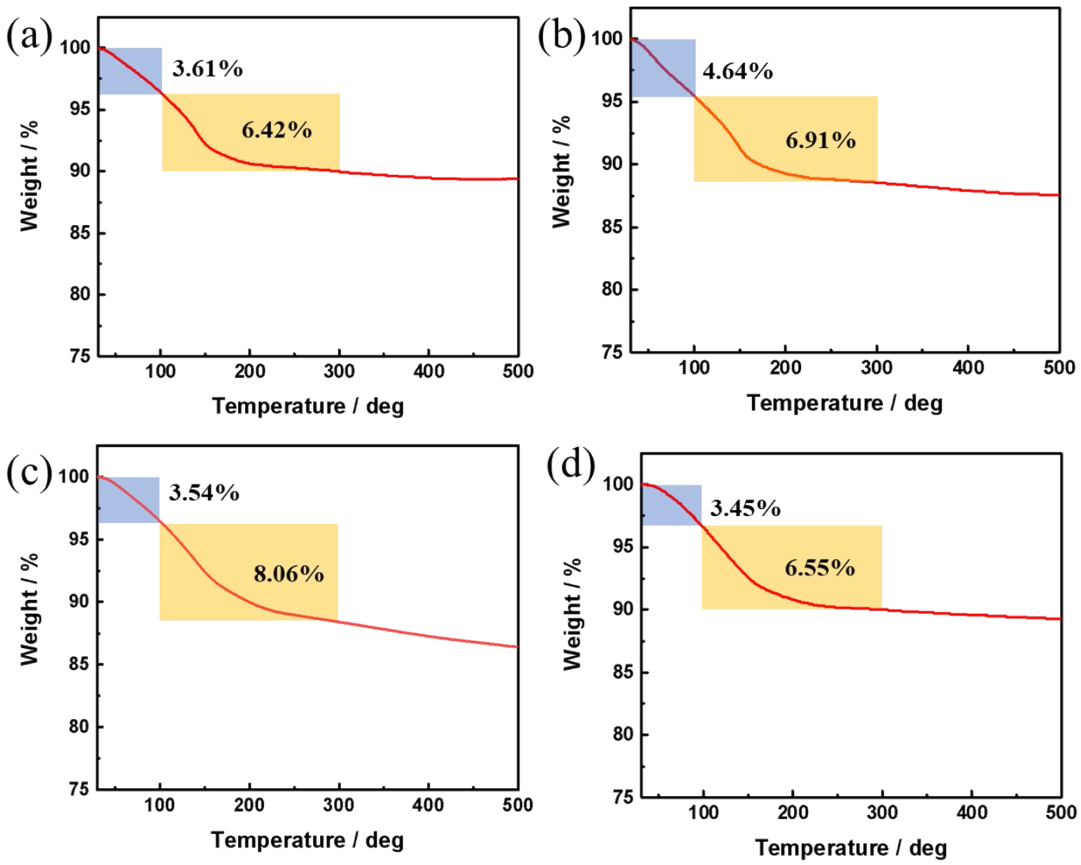

Figure S1 TGA curves of (a) MO, (b) YMO−0.05, (c) YMO−0.1, and (d) YMO−0.2.

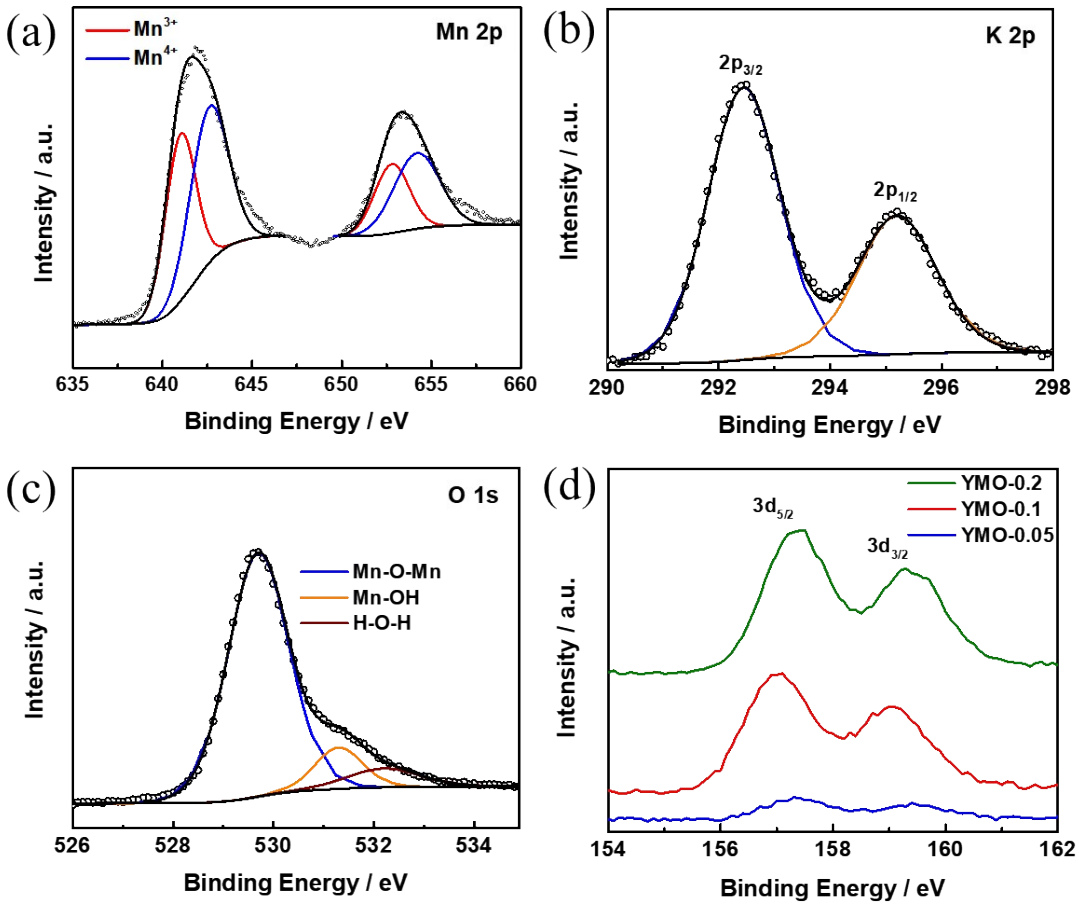

Figure S2 XPS (a) Mn 2p, (b) K 2p, and (c) O 1s spectra of MO; (d) XPS Y 3d spectra of YMO samples.

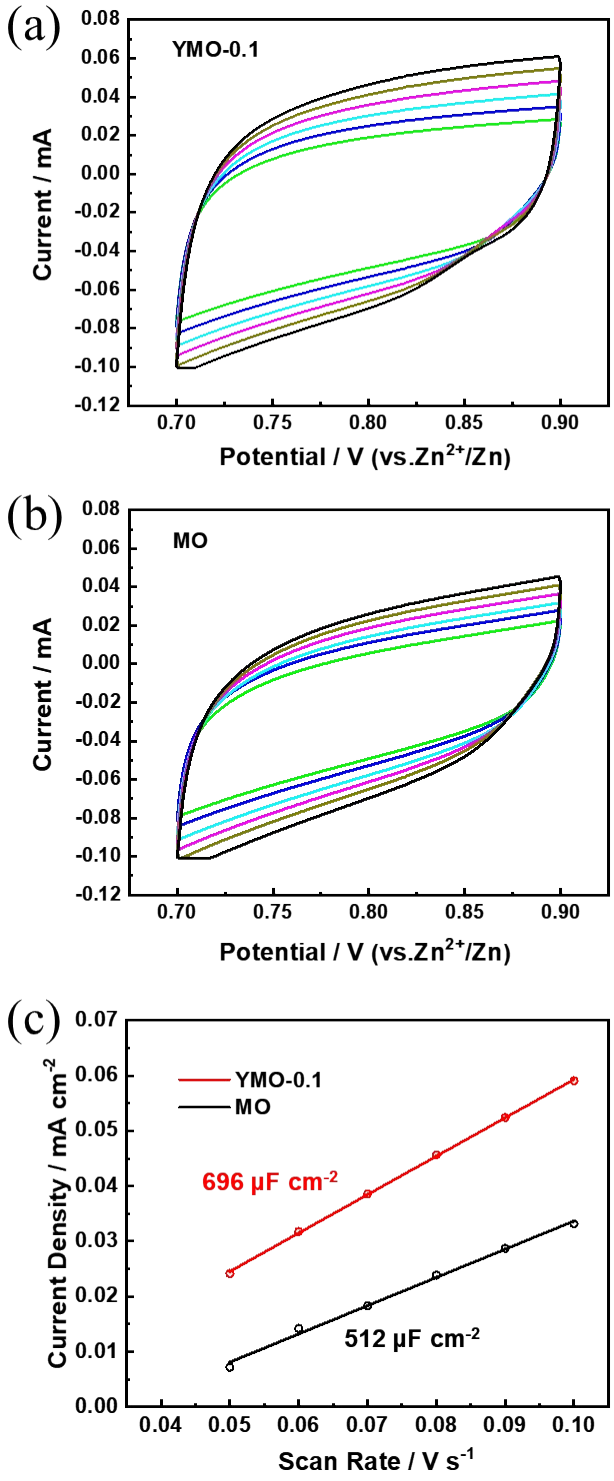

Figure S3 CV curves of (a) YMO−0.1 and (b) MO measured at the scan rate of 50−100 mV s^{-1} in the potential window between 0.7 and 0.9 V and (c) the corresponding double−layer capacitance evaluations of MO and YMO−0.1.

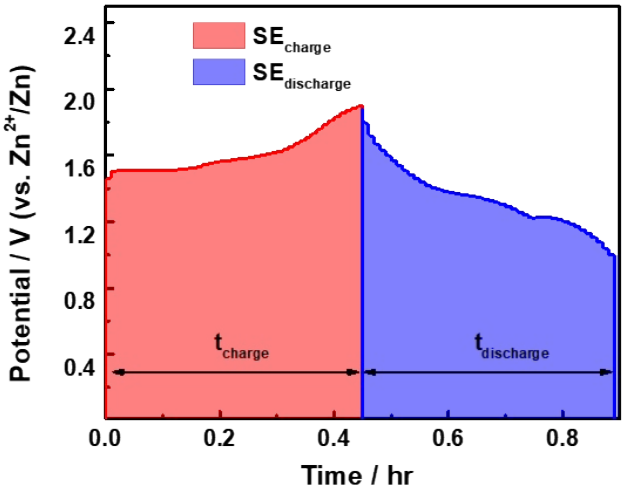

Figure S4 Evaluation of coulombic efficiency (CE), energy efficiency (EE), and specific energy for YMO−0.1 at 0.5 A g^{-1}. Specific energy (SE) can be calculated from the area under the GCD curve.

$$CE = \frac{t_{discharge}}{t_{charge}} \times 100\%$$

$$EE = \frac{SE_{discharge}}{SE_{charge}} \times 100\%$$

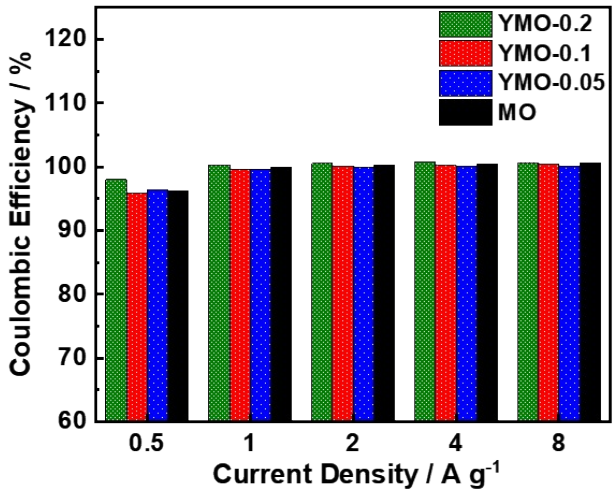

Figure S5 Coulombic efficiency evaluations of MO and YMO samples.

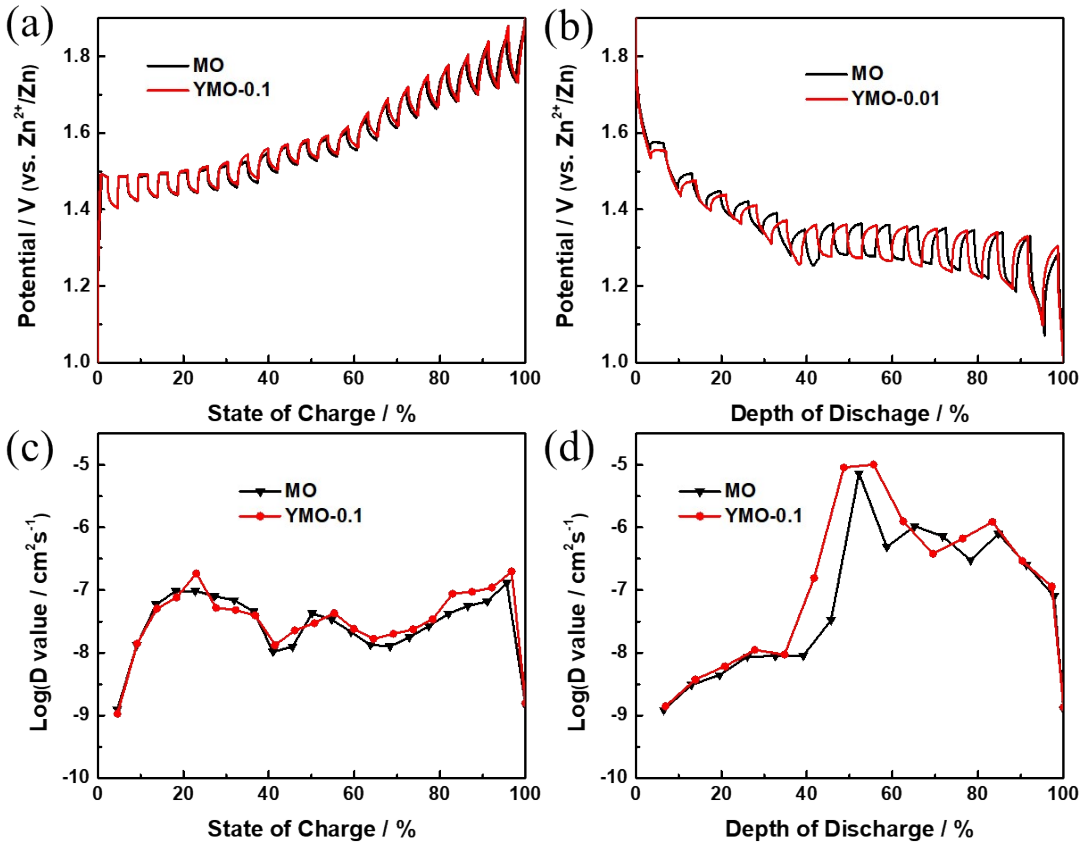

Figure S6 (a) charge and (b) discharge curves in GITT measurements and (c,d) the corresponding ion diffusion coefficient of MO and YMO−0.1.

GITT measurements were employed to evaluate solid−state ion diffusion in cathode materials based on the following equation:[1-3]

$$D = \frac{4}{\pi\tau}\left(\frac{V_M}{M_B S}\right)^2\left(\frac{\triangle E_s}{\triangle E_\tau}\right)^2$$

where τ stands for the time period for the pulse step (1800 s); V_M denotes the molar volume of the active material (103.2 cm^3 mol^{-1} based on the standard card JCPDS no. 80–1098); M_B is the molecular weight of MnO_2 (103.9 g mol^{-1} for MO and 107.8 for YMO−0.1); S is the BET surface area (112 m^2 g^{-1} for MO and 106 m^2 g^{-1} for YMO−0.1); $\triangle E_\tau$ and $\triangle E_s$ represent the voltage change (V) during titration and the difference in steady−state voltage (V) between consecutive relaxation steps, respectively.

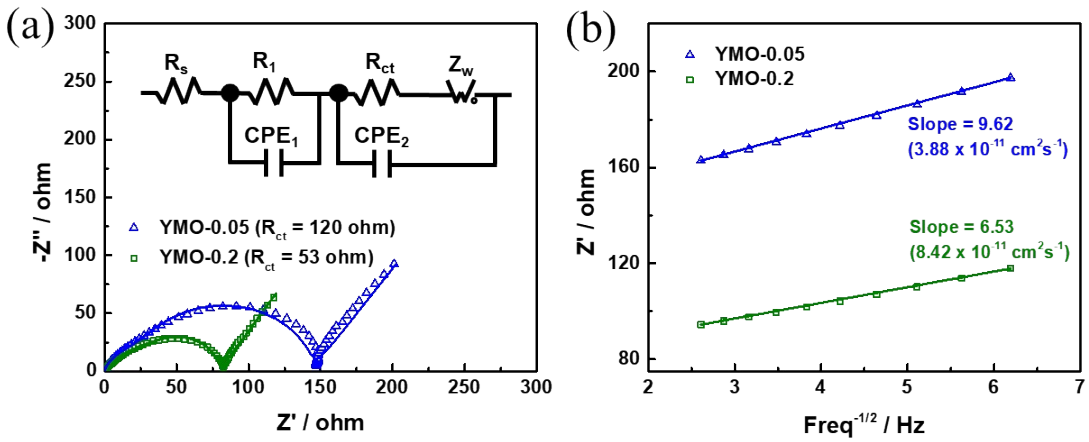

Figure S7 (a) EIS spectra and (b) Z' vs $\omega^{-0.5}$ plot of YMO−0.05 and YMO−0.2.

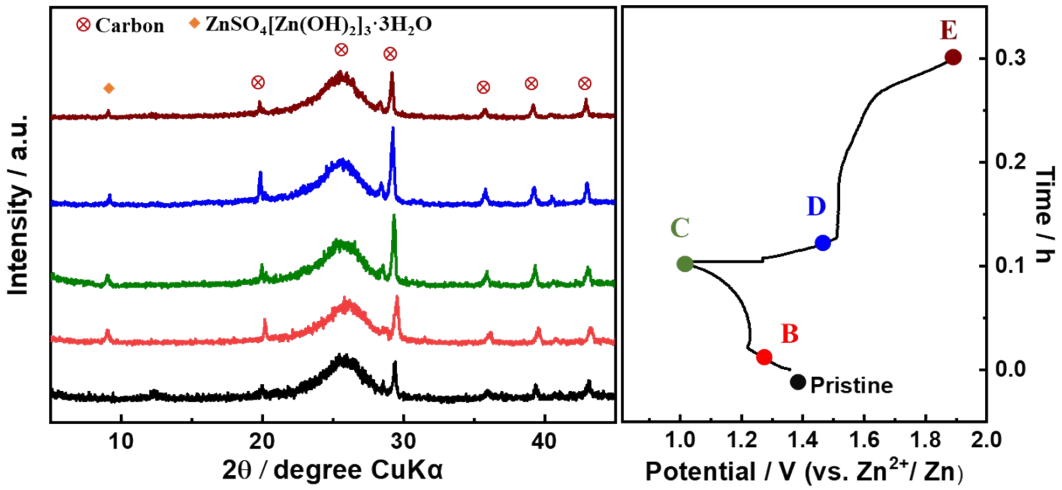

Figure S8 Ex situ XRD patterns of YMO−0.1 cathodes at various charge/discharge states.

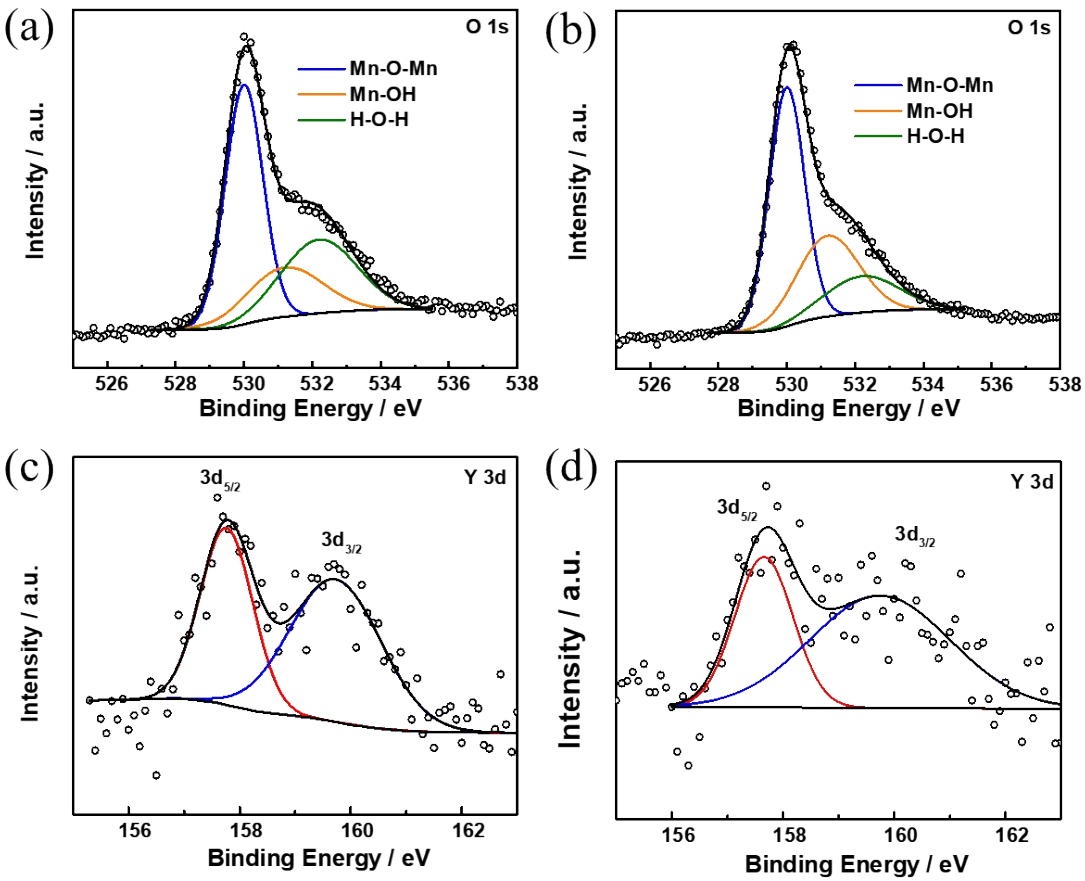

Figure S9 Ex situ XPS (a,b) O 1s and (c,d) Y 3d spectra of YMO−0.1 cathodes at (a,c) discharged state at 1.0 V and (b,d) charged state at 1.9 V.

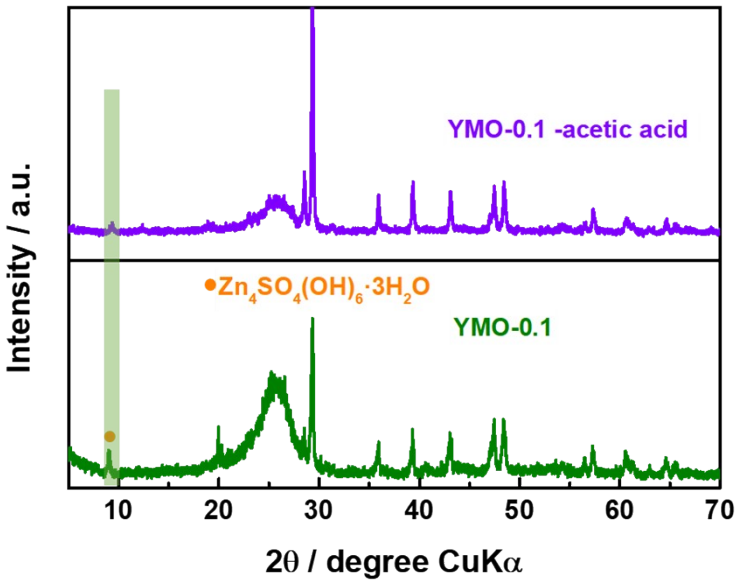

Figure S10 Comparison of XRD patterns of YMO−0.1 before and after washed with concentrated acetic acid (99.8%).

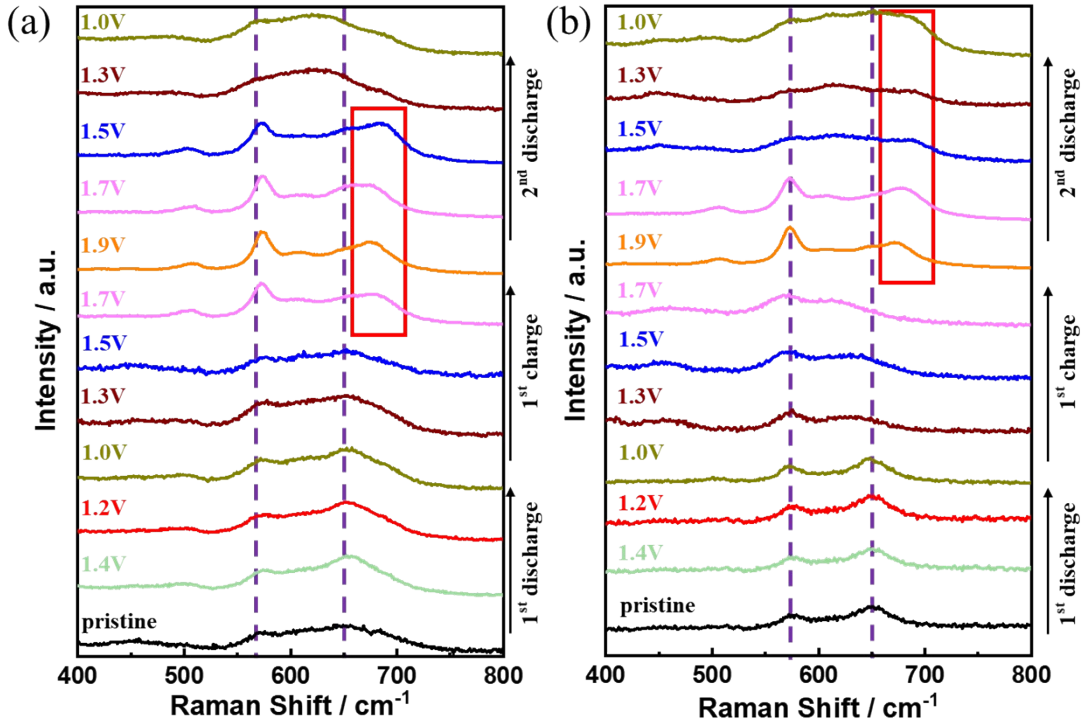

Figure S11 *In situ* Raman spectra for the 1st discharge, 1st charge, and 2nd discharge processes of (a) YMO−0.1 and (b) MO.

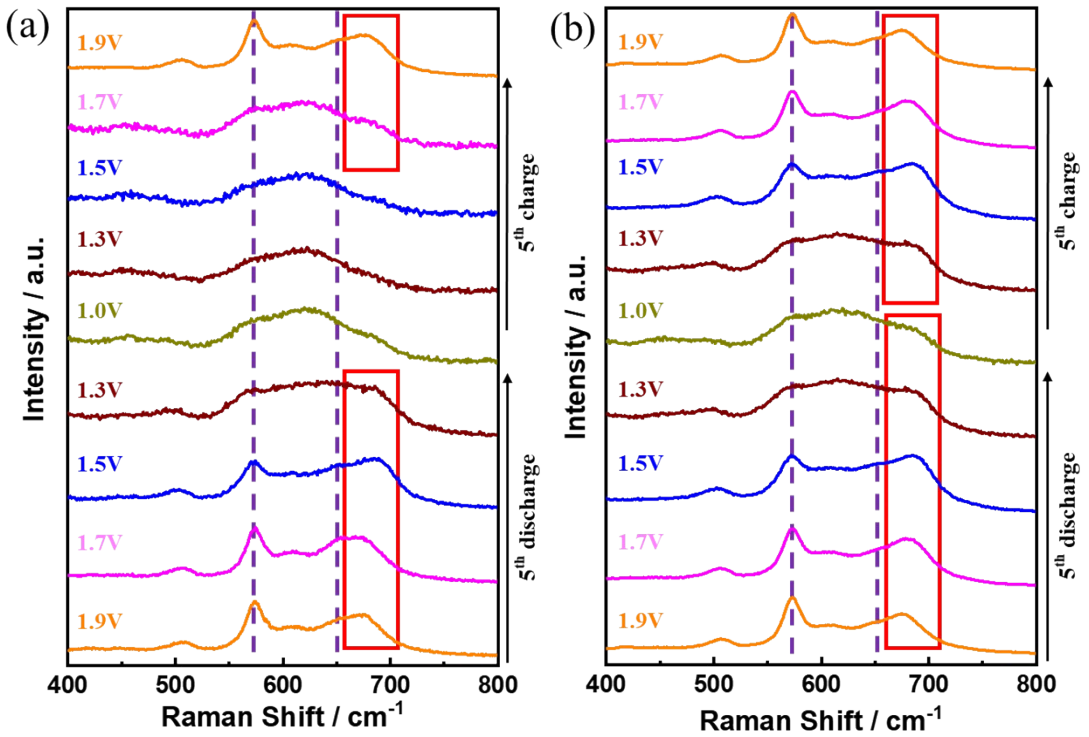

Figure S12 *In situ* Raman spectra for the 5th cycle of (a) YMO−0.1 and (b) MO.

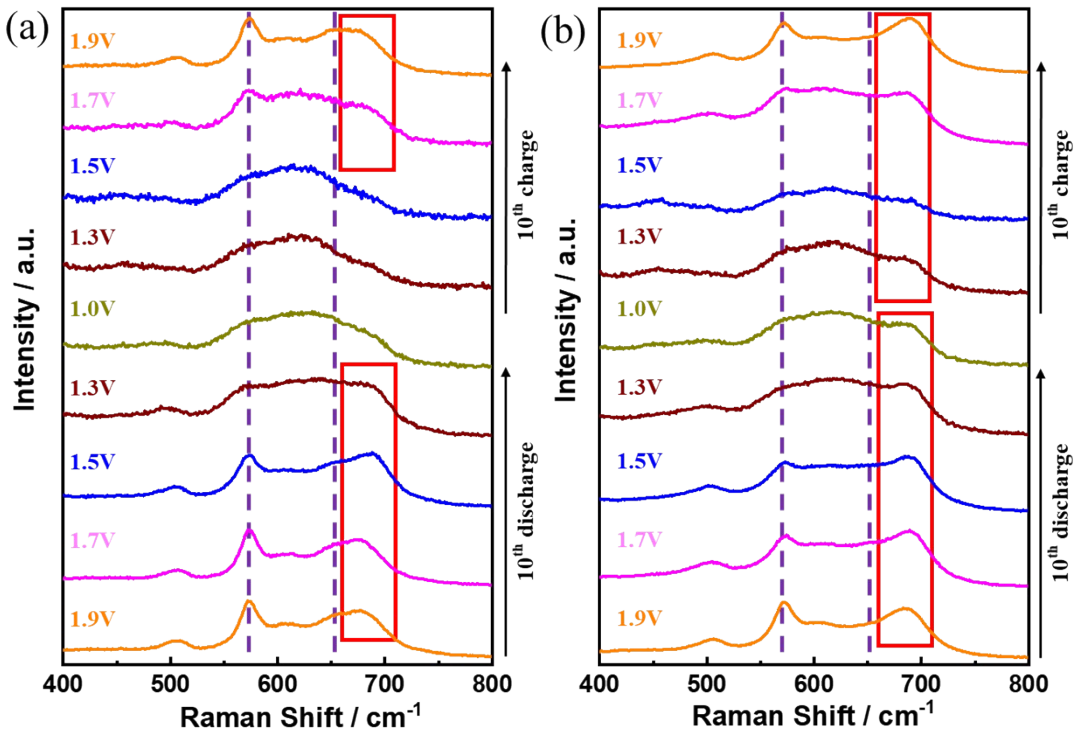

Figure S13 *In situ* Raman spectra for the 10th cycle of (a) YMO−0.1 and (b) MO.

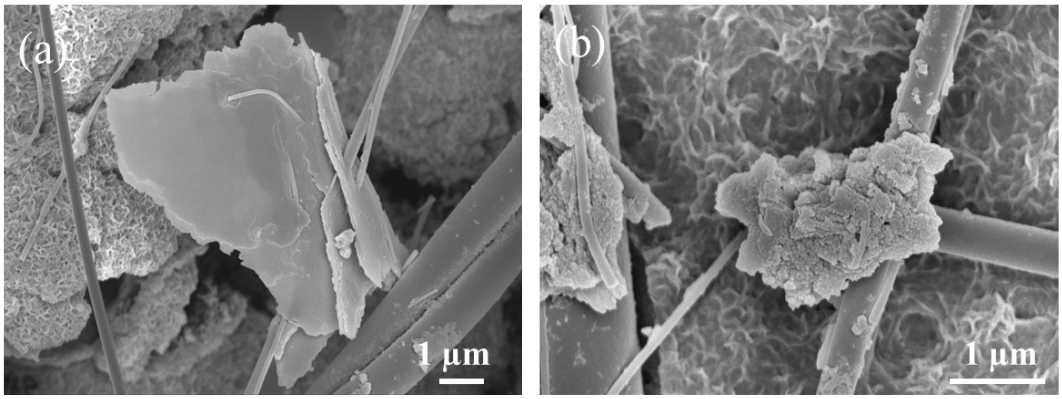

Figure S14 The SEM observations of (a) ZHS at discharged state (1.0 V) and (b) ZPM at charged state (1.9 V) of YMO−0.1 cathode without washing with concentrated acetic acid (99.8%).

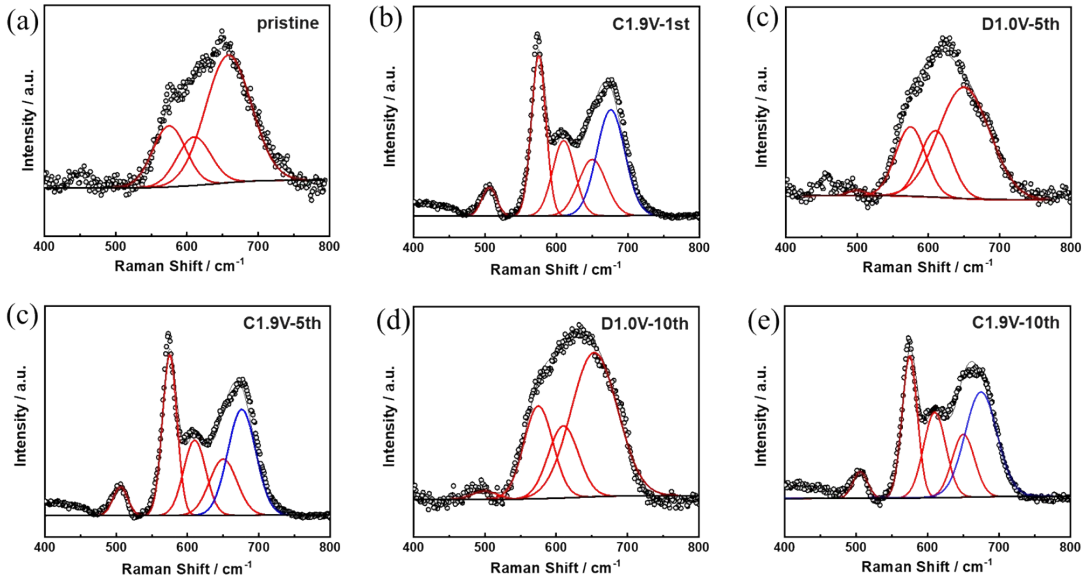

Figure S15 Lorentz fitting of Raman spectra of YMO−0.1 electrode at (a) pristine state, (b) charged to 1.9 V in the 1st cycle (C1.9V−1st), (c) discharged to 1.0 V in the 5th cycle (D1.0V−5th), (d) charged to 1.9 V in the 5th cycle (C1.9V−5th), (e) discharged to 1.0 V in the 10th cycle (D1.0V−10th), (d) charged to 1.9 V in the 10th cycle (C1.9V−10th). The blue curve corresponds to the formed Zn adsorbed phyllomanganates (ZPM).

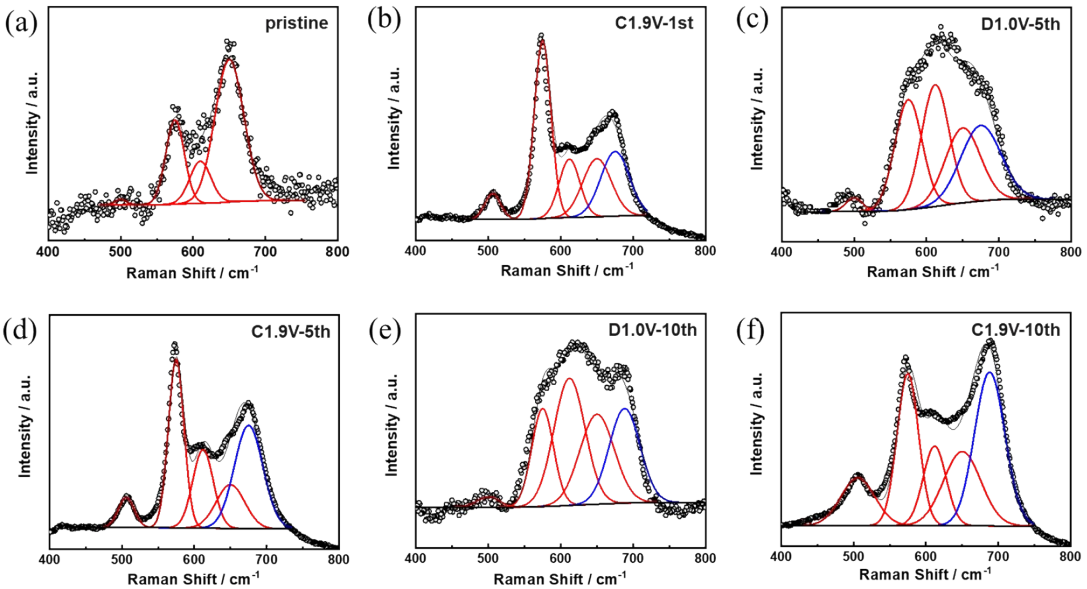

Figure S16 Lorentz fitting of Raman spectra of MO electrode at (a) pristine state, (b) C1.9V−1st, (c) D1.0V−5th, (d) C1.9V−5th, (e) D1.0V−10th, (d) C1.9V−10th. The blue curve corresponds to the formed Zn adsorbed phyllomanganates (ZPM).

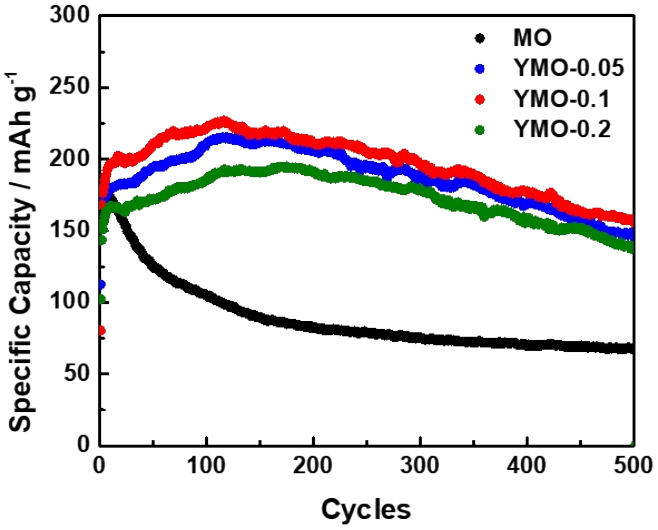

Figure S17 Cycle performance of MO and YMO samples measured at 1 A g^{-1}.

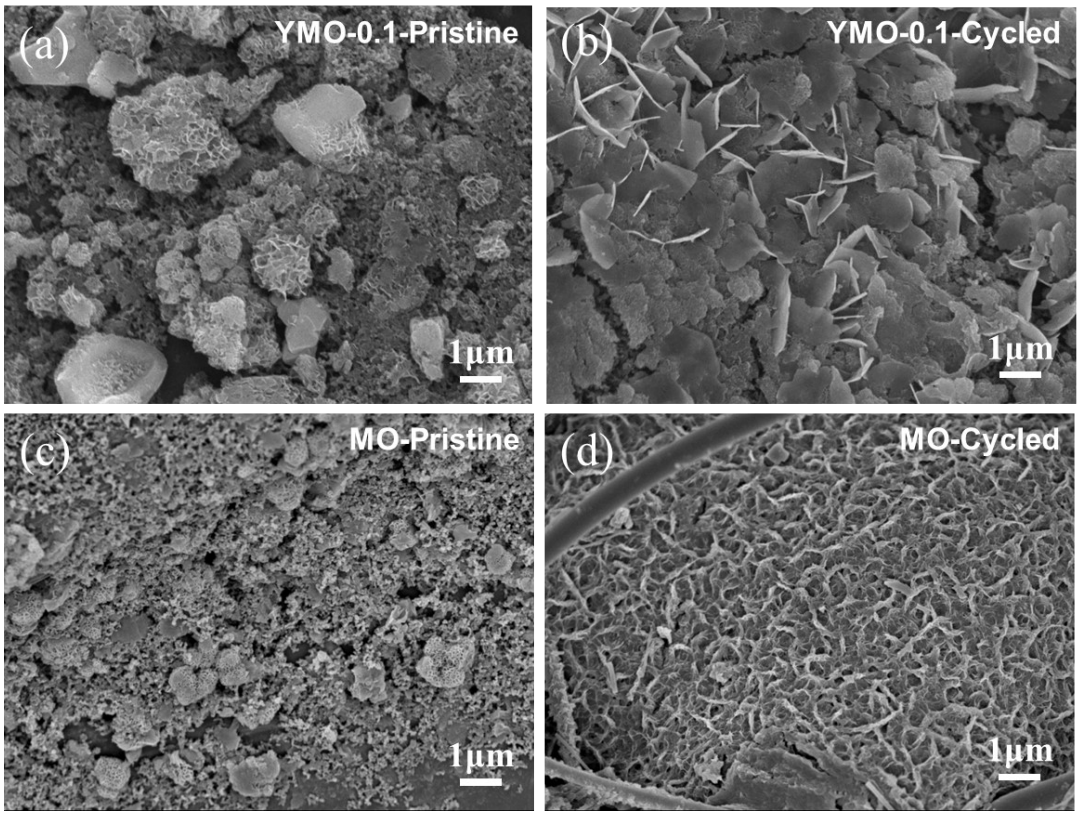

Figure S18 SEM images of (a,c) pristine and (b,d) cycled electrodes after 2000 cycles at 4 A g^{-1} stopped at 1.9 V for (a,b) YMO−0.1 and (c,d) MO.

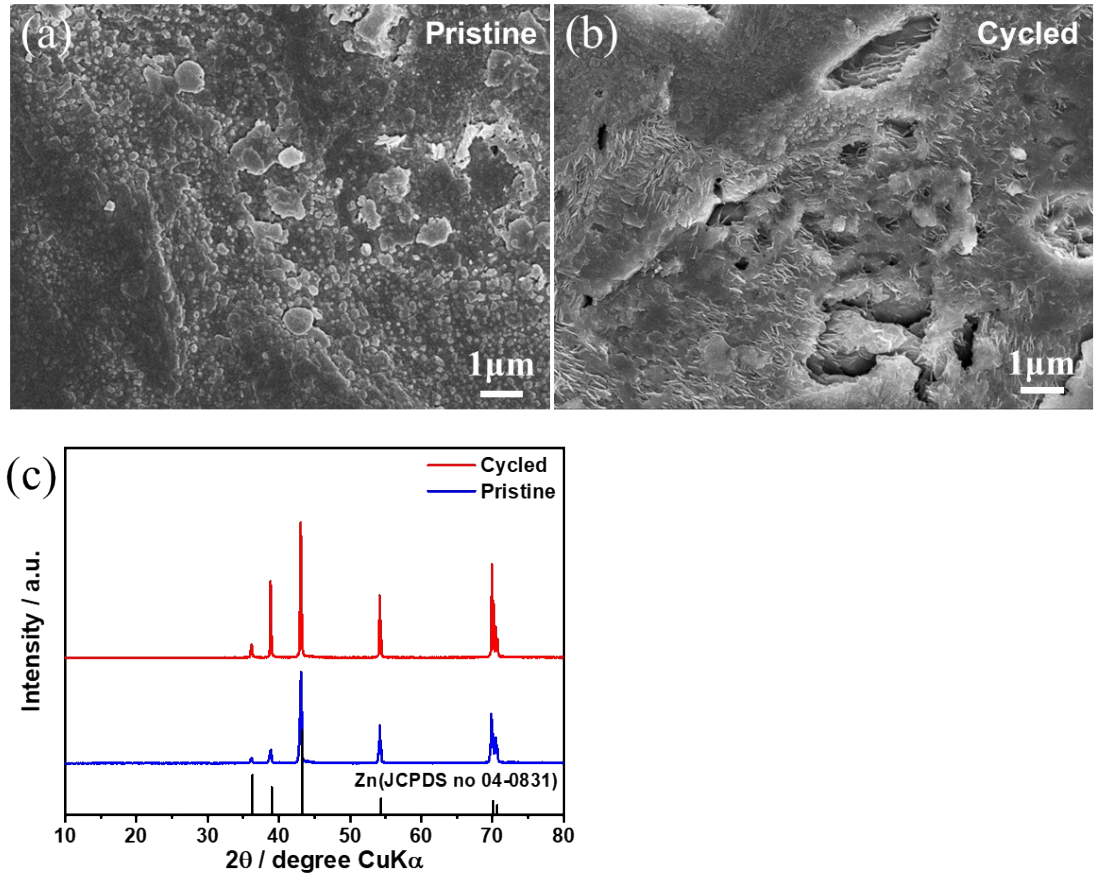

Figure S19 SEM images of (a) pristine Zn foil and (b) cycled Zn anode (paired with YMO−0.1 cathode) after 2000 cycles at 4 A g^{-1}; (c) XRD pattern of pristine and cycled Zn electrodes.

Table S1 Electrochemical performances of preintercalated metal cations layered manganese oxide cathodes used in RAZIBs.

Cathode material	Electrolyte	Voltage window (V)	Discharge capacity (mAh g^{-1})	Capacity retention / cycles / current density
$K_{0.19}Y_{0.05}MnO_2 \cdot 0.50H_2O$ nanoflakes (YMO−0.1)	**1 M $ZnSO_4$ + 0.1 M $MnSO_4$**	**1.0~1.9**	**212 at 0.5 A g^{-1} 143 at 2.0 A g^{-1} 114 at 4.0 A g^{-1}**	**95% / 3000 / 4.0 A g^{-1}**
Sn^{4+}−MnO_2/SnO_2 nanosheets[4]	2 M $ZnSO_4$ + 0.1 M $MnSO_4$	0.8~1.8	279.6 at 0.5 A g^{-1} 179.4 at 2.0 A g^{-1}	92.4 % / 2000 / 2.0 A g^{-1}
K^+/Al^{3+}−MnO_2 nanosheets[5]	2 M $ZnSO_4$ + 0.1 M $MnSO_4$	0.8~1.9	269.5 at 0.5 A g^{-1} 85.2 at 2.0 A g^{-1}	76% / 300 / 0.5 A g^{-1}
Bi^{3+}−MnO_2 nanoflower[6]	2 M $ZnSO_4$ + 0.1 M $MnSO_4$	0.8~1.9	130.8 at 0.4 A g^{-1} 65.9 at 2.0 A g^{-1}	98.6% / 1100 / 1.0 A g^{-1}
Co^{3+}−MnO_2 thin film[7]	1 M $ZnSO_4$ + 0.07 M $MnSO_4$	1.0~1.8	288 at 0.3 A g^{-1} 205 at 3.0 A g^{-1}	~100 % / 600 / 1.2 A g^{-1}
La^{3+}−MnO_2	1 M $ZnSO_4$ +	0.8~1.9	279 at 0.1 A g^{-1}	71% / 200 / 0.2 A g^{-1}

nanoflorets[8]	0.4 M $MnSO_4$		122 at 1.6 A g^{-1}	
Zn^{2+}–MnO_2 nanospheres[9]	2 M $ZnSO_4$ + 0.1 M $MnSO_4$	0.8~1.9	272 at 0.3 A g^{-1} 121 at 3.0 A g^{-1}	72% / 2000 / 3.0 A g^{-1}
Cu^{2+}–MnO_2 nanoflakes[10]	1 M $ZnSO_4$ + 0.1 M $MnSO_4$	1.0~1.9	240 at 0.5 A g^{-1} 121 at 4.0 A g^{-1}	99% / 1500 / 4.0 A g^{-1}
Ca^{2+}–MnO_2 nanoflakes[11]	1 M $ZnSO_4$ + 0.1 M $MnSO_4$	0.4~1.9	277.7 at 0.35 A g^{-1} 124.5 at 3.5 A g^{-1}	~80 % /5000 / 3.5 A g^{-1}
K^{+}–MnO_2 nanoflakes[12]	2 M $ZnSO_4$ + 0.2 M $MnSO_4$	0.4~1.9	425 at 0.175 A g^{-1} 108 at 3.5 A g^{-1}	93 % / 1500 / 3.5 A g^{-1}
Na^{+}–Mn_2O_4 nanoplates[13]	2 M $ZnSO_4$ + 0.2 M $MnSO_4$	0.9~1.9	232 at 0.616 A g^{-1} 134 at 3.08 A g^{-1}	98% / 10000 /6.16 A g^{-1}

References

1. N. Zhang, F. Cheng, Y. Liu, Q. Zhao, K. Lei, C. Chen, X. Liu and J. Chen, *J. Am. Chem. Soc.*, 2016, **138**, 12894-12901.
2. N. Zhang, M. Jia, Y. Dong, Y. Wang, J. Xu, Y. Liu, L. Jiao and F. Cheng, *Adv. Funct. Mater.*, 2019, **29**, 1807331.
3. Y. Dong, S. Di, F. Zhang, X. Bian, Y. Wang, J. Xu, L. Wang, F. Cheng and N. Zhang, *J. Mater. Chem. A*, 2020, **8**, 3252-3261.
4. S. Wang, W. Ma, Z. Sang, F. Hou, W. Si, J. Guo, J. Liang and D. a. Yang, *J. Energy Chem.*, 2022, **67**, 82-91.
5. S. Zhou, X. Wu, H. Du, Z. He, X. Wu and X. Wu, *J. Colloid Interface Sci.*, 2022, **623**, 456-466.
6. F. Long, Y. Xiang, S. Yang, Y. Li, H. Du, Y. Liu, X. Wu and X. Wu, *J. Colloid Interface Sci.*, 2022, **616**, 101-109.
7. F. Kataoka, T. Ishida, K. Nagita, V. Kumbhar, K. Yamabuki and M. Nakayama, *ACS Appl. Energy Mater.*, 2020, **3**, 4720-4726.
8. H. Zhang, Q. Liu, J. Wang, K. Chen, D. Xue, J. Liu and X. Lu, *J. Mater. Chem. A*, 2019, **7**, 22079-22083.
9. J. Wang, J.-G. Wang, H. Liu, C. Wei and F. Kang, *J. Mater. Chem. A*, 2019, **7**, 13727-13735.
10. T. H. Wu, W. Y. Liang and Y. Q. Lin, *J. Taiwan Inst. Chem. Eng.*, 2022, **131**, 104172.
11. T. Sun, Q. Nian, S. Zheng, J. Shi and Z. Tao, *Small*, 2020, **16**, 2000597.
12. T. Sun, Q. Nian, S. Zheng, X. Yuan and Z. Tao, *J. Power Sources*, 2020, **478**, 228758.
13. D. Wang, L. Wang, G. Liang, H. Li, Z. Liu, Z. Tang, J. Liang and C. Zhi, *ACS Nano*, 2019, **13**, 10643-10652.